Experimental observation of response to resonant magnetic perturbation and its hysteresis in LHD

2015 Nucl. Fusion 55 073004

(http://iopscience.iop.org/0029-5515/55/7/073004)

OPEN ACCESS
IOP Publishing | International Atomic Energy Agency Nuclear Fusion
Nucl. Fusion **55** (2015) 073004 (7pp) doi:10.1088/0029-5515/55/7/073004

Experimental observation of response to resonant magnetic perturbation and its hysteresis in LHD

Y. Narushima[1,2], S. Sakakibara[1,2], S. Ohdachi[1,2], Y. Suzuki[1,2], K.Y. Watanabe[1], S. Nishimura[3], S. Satake[1,2], B. Huang[2], M. Furukawa[4], Y. Takemura[1], K. Ida[1,2], M. Yoshinuma[1,2], I. Yamada[1] and The LHD Experiment Group[1]

[1] National Institute for Fusion Science, 322–6 Oroshi-cho, Toki-city, Gifu, 509-5292, Japan
[2] Sokendai, The Graduate University for Advanced Studies, 322-6 Oroshi-cho, Toki-city, Gifu, 509-5292, Japan
[3] Kobe City College of Technology, 8-3 Gakuen-Higashi-machi, Nishi-ku, Kobe-city, Hyogo, 651-2194, Japan
[4] Tottori University, 4-101 Koyama-cho minami, Tottori-city, Tottori, 680-8550, Japan

E-mail: narusima@LHD.nifs.ac.jp

Received 19 December 2014, revised 8 May 2015
Accepted for publication 8 May 2015
Published 5 June 2015

Abstract

The magnetic island in the large helical device (LHD) shows the dynamic behaviour of the healing/growth transition with the hysteretic behaviour. The thresholds of plasma beta and poloidal flow for island healing are larger than that for growth. The threshold of resonant magnetic perturbation (RMP) for healing is smaller than that for growth. Furthermore, thresholds of the amplitude of RMP depend on the magnetic axis position R_{ax} in the LHD. The RMP threshold increases as the magnetic axis position R_{ax} increases. The poloidal viscosity may be considered as a candidate to explain the experimental observation from the viewpoint of the relationship between the electromagnetic torque and the viscous torque.

Keywords: halical plasma, magnetic island, plasma response

1. Introduction

For the good confinement of toroidal plasmas, nested flux surfaces are required. However, magnetic islands can be generated by an error field produced by various means. A small magnetic island might trigger a magnetohydrodynamic (MHD) instability called neoclassical tearing mode which leads to a deterioration of the confinement and may possibly lead to a locked mode in Tokamak plasmas [1], whereas a serious disruption never occurs even if the magnetic island grows in the large helical device (LHD) plasmas. The magnetic islands intrinsically disappear as they are stabilised during a plasma discharge under certain conditions [2, 3] and the grown magnetic island merely triggers a minor collapse when the magnetic shear becomes low [4]. According to the circumstances, a detached state can be induced by the growth of the magnetic island at the peripheral region [5], which implies an advantage in utilising a magnetic island. In an effort to investigate the behaviour of islands, the LHD has performed a set of experiments in which resonant magnetic perturbation (RMP) coils are intentionally applied to produce a large magnetic island chain at a low-order rational surface. The RMP coils make a vacuum magnetic island with $m/n = 1/1$ (here, m/n is the poloidal/toroidal Fourier mode number) structure. Recent study has found that the magnetic island shows nonlinear growth or suppression during a discharge and that the dynamics of the magnetic island are affected by the poloidal plasma rotation [6]. It is thought that the production and control of optimised magnetic islands deliver significant benefit to obtain high-performance plasmas. Therefore, the study of the dynamics of magnetic islands has been a critical issue. This article is composed as follows. In the following section, the experimental setup is introduced. The experimental observations are shown in section 3. Section 4 shows the discussion. Finally, the summary is given in section 5.

2. Experimental setup of LHD

The distinguishing feature of the heliotron-type plasma confinement device LHD is the presence of a set of continuous

helical coils with a poloidal/toroidal winding number 2/10. The helical and poloidal coils used to confine the plasma are superconducting. Ten pairs of coils made of normal conductors set at the top and bottom of the LHD can produce a magnetic field with $m/n = 1/1$ and/or 2/1 modes. In this study, to make the magnetic island with $m/n = 1/1$, the perturbation field is imposed by RMP coils. In addition, the other RMP coils are also used to cancel the toroidal coupling component of $m/n = 2/1$. Typical major and averaged minor radii of the plasmas are $R = 3.9$ m and $a = 0.5$ m, respectively. The rotational transform ($\iota/2\pi$) profile is monotonically increasing with a radius with axis values near $\iota/2\pi \sim 0.4$ and edge value $\iota/2\pi \sim 1$ in the vacuum configuration.

3. Experimental result

Shown in this section are the previous and present experimental observations of the magnetic island in the LHD in which the island behaviour in the quasi-steady state and the transient state are included.

3.1. Island behaviour in quasi-steady state

Under the magnetic configuration with the vacuum magnetic island produced by the static RMP with $m/n = 1/1$, the plasma tends to make the island grow (be healed) in width at low (high) beta and high (low) collisionality, as shown in figure 1. The beta and collisionality are the local value at the rational surface of $\iota/2\pi = 1$. Here, the collisionality of $\nu^*_{\rm heff}$ is defined as the collisionality normalised by the effective helical ripple $\varepsilon_{\rm heff}$ ($\nu^*_{\rm heff} = \nu_e/\{\epsilon^{3/2}_{\rm heff}(\iota/2\pi)(v_{\rm Th}/R)\}$). It can be seen that the region of growth (plotted by closed circles) is enlarged for high RMP current condition and vice versa. While beta and collisionality can correlate with island physics through Pfirsch-Schlüter (PS) and bootstrap (BS) current effects, efforts to understand these results via these mechanisms failed [3]. In the previous experiment [3], the magnetic island states (growth and healing) can be divided into two regions in the beta and collisionality space, as shown in figure 1. The island behaviour correlates to beta and collisionality in experiment. However, the boundary line written in figure 1 cannot be explained by the theoretically obtained PS and BS current effect. Authors thus have realised that some other mechanisms should exist. The transitional phenomenon was focused on clarifying the behaviour of the magnetic island.

3.2. Transition of magnetic island

The data plotted in figure 1 were acquired from the quasi-steady state, in which the vacuum magnetic islands experience the saturated grown island or suppression transited from growth. Here, one is interested in the transition of the magnetic island. To clarify the behaviour of magnetic island showing the transition, parameters of the poloidal flow and the RMP are changed during a single discharge.

3.2.1. Dependence of plasma beta. Figure 2 shows the waveform in which the magnetic island shows double transitions in a single discharge. In the beginning of the discharge at $t \leqslant 4$ s, the magnetic island shows growth ($w > w_{\rm vac}$) here, w ($w_{\rm vac}$) means the width of the (vacuum) island. The $w_{\rm vac}$ is drawn by a dashed line in figure 2(f). When the additional neutral beam injection (NBI) is injected at $t = 4.1$ s, the β increases prior to the island suppression ($w = 0$) at $t = 4.4$ s. After that, the magnetic island shows regrowth ($w > w_{\rm vac}$) at $t = 4.8$ s after the β decreases by turned off NBI. The relationship between the phase difference, $\Delta\theta_{m=1}$, and the β is shown in figure 3 in which arrows indicate the time trend. Here, the phase difference ($\Delta\theta_{m=1}$) is defined as the difference of the phase between the plasma response and the RMP. When the phase difference is zero ($\Delta\theta_{m=1} = 0$), the magnetic island grows, and when it is out of phase ($\Delta\theta_{m=1} = \pi$), the magnetic island is suppressed. When the β increases, $\Delta\theta_{m=1}$ goes from 0 to $\Delta\theta_{m=1} = -\pi$ (rad) and finally the island is suppressed at $\beta = 0.3\%$. On the other hand, $\Delta\theta_{m=1}$ returns to $\Delta\theta_{m=1} = 0$ (growth) at $\beta = 0.1\%$. The β for island suppression (0.3%) is larger than that for island regrowth (0.1%). These experimental results show the existence of a beta hysteresis in the magnetic island transition dynamics, i.e., once the magnetic island is suppressed by increasing beta, it lasts until the beta becomes sufficiently small.

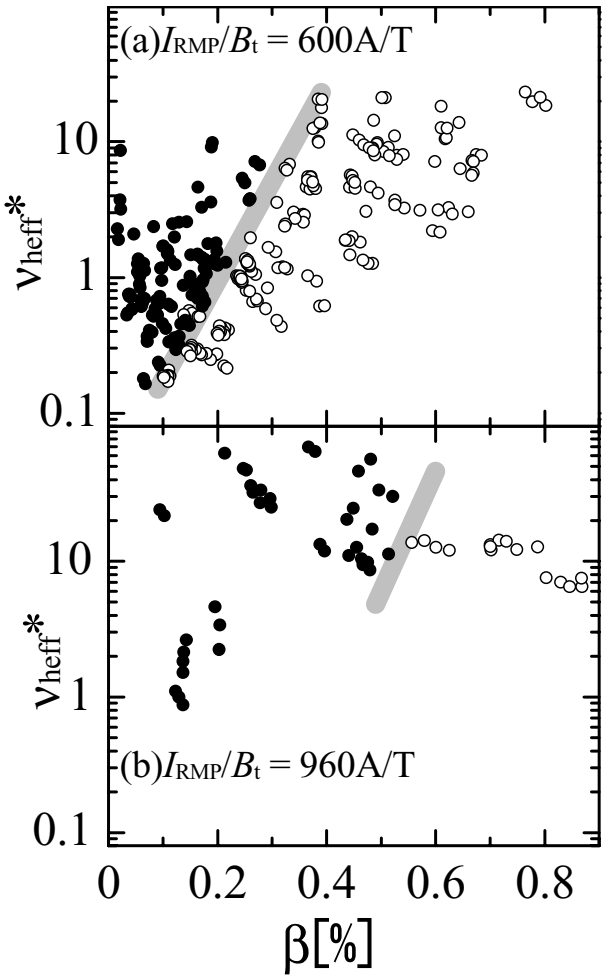

Figure 1. Island growing (closed) and suppressing (open) region in β–ν space. Boundary is drawn by gray solid line. Normalised RMP coil current is (a) 600 A/T and (b) 960 A/T.

3.2.2. Effect of poloidal flow. A recent study has found that the dynamics of the magnetic island is affected by the

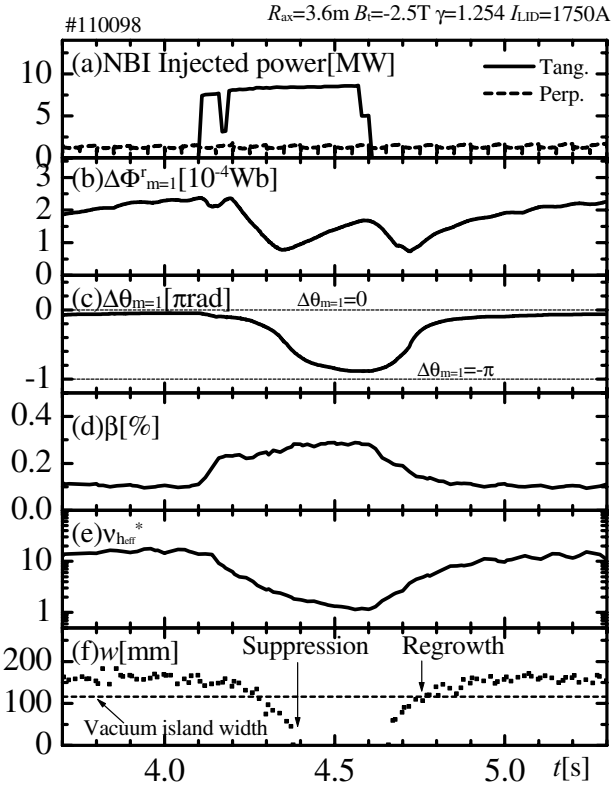

Figure 2. Time evolution of (*a*) NBI power, (*b*) plasma response field, (*c*) phase shift, (*d*) plasma beta, (*e*) collisionality, and (*f*) island width. Vacuum island width is indicated by the dashed line.

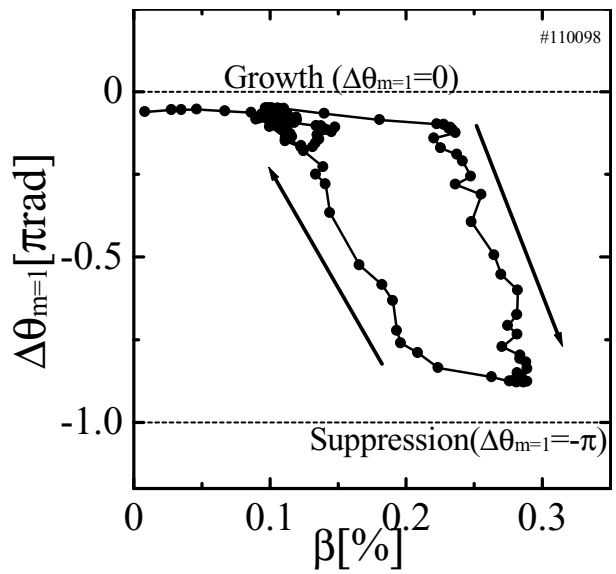

Figure 3. Relationship between phase shift ($\Delta\theta_{m=1}$) and beta. Time evolution is indicated by arrows.

poloidal plasma rotation [6], which shows the experimental fact that the poloidal flow increases (decreases) prior to the healing (growth) transition of magnetic island. Figure 4 (near replication of figure 3 in [6]) shows the minor radius profile of electron temperature (T_e, closed circles) measured by Thomson scattering and the poloidal flow (ω_{pol}, open

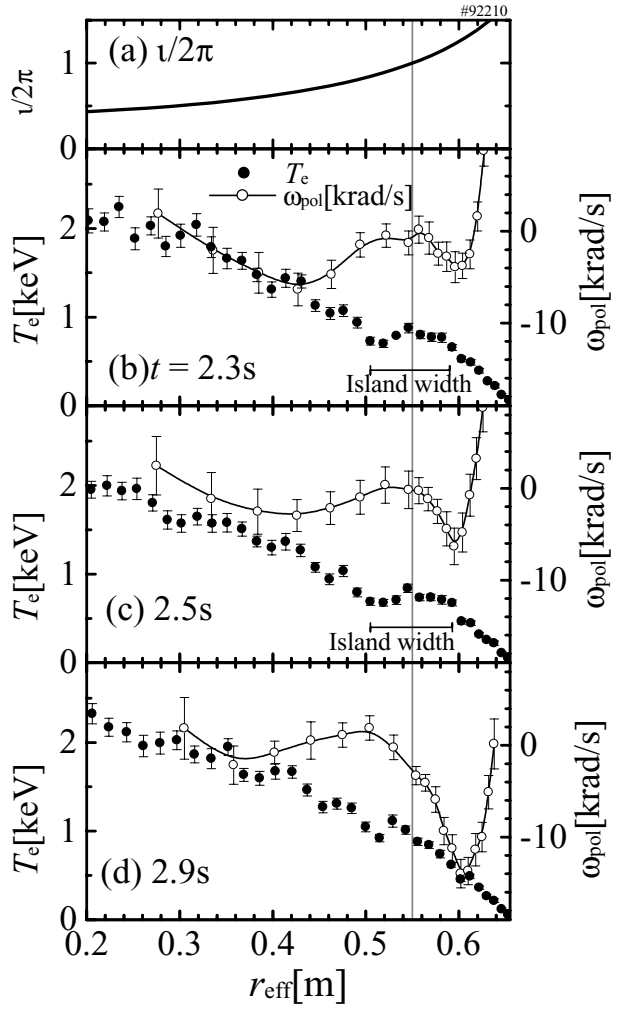

Figure 4. Radial profile of (*a*) $\iota/2\pi$, (*b–d*) T_e (closed), and ω_{pol} flow (open). The island (local flattening at $r_{eff} \sim 0.55$ m) transits from growth to healing. The $|\omega_{\boldsymbol{E}\times\boldsymbol{B}}|$ at $r_{eff} \sim 0.6$ m increases with time prior to the island being healed.

circles) measured by charge exchange spectroscopy (CXS). The negative sign of ω_{pol} indicates the electron diamagnetic direction; the poloidal flow is always in this direction in this study. The resonant surface of $\iota/2\pi = 1$ lies at $r_{eff} = 0.55$ m. To control the poloidal flow, the plasma parameters of beta and collisionality are changed by varying the NBI power, B_t, and electron density. The NBI power was increased to 11 from 9.7 MW. As a result, the beta was changed to 0.24 from 0.17%. The local flattening of the T_e profile indicates the existence of the magnetic island, as shown in figures 4(*b*) and (*c*). Later in the discharge, the island disappears (figure 4(*d*)). During the magnetic island healing, the absolute value of the poloidal flow $|\omega_{pol}|$ in the electron-diamagnetic direction lying at $r_{eff} = 0.6$ m increases with time and its profile becomes wide. Figure 5 shows the relationship between the phase difference, $\Delta\theta_{m=1}$, and the poloidal flow, ω_{pol}, at just outside the $\iota/2\pi = 1$, in which arrows indicate the time trend. In the case of the transition from growth to suppression (figure 5(*a*)) the phase shift $\Delta\theta_{m=1} = 0$ transits from $\Delta\theta_{m=1} \sim -0.1\pi$ (rad) to $\Delta\theta_{m=1} \sim -\pi$ (rad). The threshold value of the poloidal flow, ω_{pol}^{th}, derived from the

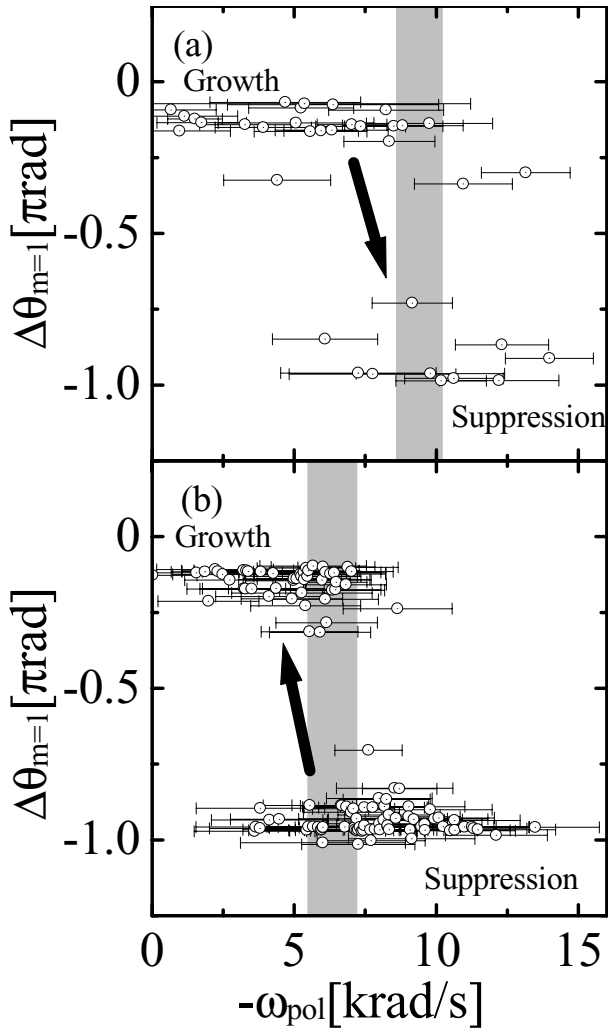

Figure 5. Relationship between $\Delta\theta_{m=1}$ and ω_{pol}. Case of (*a*) growth to suppression, (*b*) suppression to growth. Arrows indicate time trend. Grey solid line indicates threshold of poloidal rotation for transition ($\omega^{\mathrm{th}}_{\mathrm{pol}}$). Threshold values of poloidal rotation are (*a*) $\omega^{\mathrm{th}}_{\mathrm{pol}} = -9.4 \pm 0.8$ krad s^{-1} and (*b*) $\omega^{\mathrm{th}}_{\mathrm{pol}} = -6.4 \pm 0.9$ krad s^{-1}, respectively.

fitting of a Heaviside-function is $\omega^{\mathrm{th}}_{\mathrm{pol}} = -9.4 \pm 0.8$ krad s^{-1}. In the other case of the transition from suppression to growth (figure 5(*b*)), $\omega^{\mathrm{th}}_{\mathrm{pol}} = -6.4 \pm 0.9$ krad s^{-1}. These experimental results show the existence of a poloidal flow hysteresis in the magnetic island transition dynamics: when the magnetic island is suppressed by the high poloidal flow one time, the suppression lasts until the poloidal flow becomes small enough. This is an advantageous behaviour from the viewpoint of the magnetic island stabilisation.

3.2.3. Effect of time-varying RMP. In the experimental observations mentioned above, the plasma originated parameters (plasma beta, poloidal flow) are controlled to obtain the transition of the magnetic island. Hereafter, the magnetic configuration originated parameters are changed.

Figure 6 shows the typical waveforms of an $m/n = 1/1$ amplitude of RMP $\Delta\Phi_{\mathrm{RMP}}$, amplitude of plasma response field of resonant Fourier mode $\Delta\Phi_{m=1}$, and phase difference between RMP and the plasma response field $\Delta\theta_{m=1}$ in the configuration with $R_{\mathrm{ax}} = 3.75$ m. Here, $\Delta\Phi_{\mathrm{RMP}}$ and $\Delta\Phi_{m=1}$ have the unit of (Wb) because they are detected by non-planar flux loops [7]. In the case in which the RMP is ramped up during the discharge (left row in figure 6), the phase difference $\Delta\theta_{m=1}$ is $\Delta\theta_{m=1} = -\pi$ (rad) (which means the RMP is shielded) until $t = 5.83$ s (figure 6(*c*)). In this period the plasma response field $\Delta\Phi_{m=1}$ increases linearly with ramped $\Delta\Phi_{\mathrm{RMP}}$, which compensates the RMP field. As a result, the magnetic island shows healing. The T_{e} profile does not have the local flattening region (imposed in figure 6(*c*)). After $t = 5.83$ s, the phase difference moves from $\Delta\theta_{m=1} = -\pi$ (rad) which means the RMP penetrates into the plasma and the local flattening appears in the T_{e} profile at $R = 3.1$ m (in figure 6(*c*)). In the case of ramping down RMP (right row in figure 6), the $\Delta\theta_{m=1}$ deviates from $\Delta\theta_{m=1} = -\pi$ (rad) until $t = 4.3$ s (figure 6(*f*)) and local flattening of T_{e} (imposed in figure 6(*f*)) indicates the island formation. And then the RMP is shielded after $t = 4.3$ s and local flattening disappears (imposed in figure 6(*f*)).

3.3. Dependence of the threshold of RMP to transition on the magnetic axis position

The dependence of the critical normalised $\Delta\Phi_{\mathrm{RMP}}$ for these transitions on the magnetic axis position R_{ax} are shown in figure 7. Here, the *critical* normalised $\Delta\Phi_{\mathrm{RMP}}$ means the threshold of the $\Delta\Phi_{\mathrm{RMP}}$ for the transition. The critical $\Delta\Phi_{\mathrm{RMP}}$ increases with R_{ax} in both cases. The larger $\Delta\Phi_{\mathrm{RMP}}$ is required in the configuration with larger R_{ax} for both transitions (healing to growth / growth to healing). In the case of the RMP ramp up (figure 7(*a*)), the critical $\Delta\Phi_{\mathrm{RMP}}$ at $R_{\mathrm{ax}} = 3.8$ m is 2.5 times larger than that in $R_{\mathrm{ax}} = 3.6$ m. Similarly, the critical $\Delta\Phi_{\mathrm{RMP}}$ at $R_{\mathrm{ax}} = 3.8$ m is three times larger than that in $R_{\mathrm{ax}} = 3.6$ m in the case of the RMP ramp down (figure 7(*b*)). This experimental observation means that the magnetic configuration with larger magnetic axis position tends to possess a robustness to the external imposed error field to retain the nested flux surfaces. It is also found that the critical $\Delta\Phi_{\mathrm{RMP}}$ for the case of ramp-up (figure 7(*a*)) is larger than that of the ramp-down case (figure 7(*b*)). The nature of hysteresis provides that once the magnetic island is produced at a certain critical value by an increase in RMP, lower critical $\Delta\Phi_{\mathrm{RMP}}$ is required to suppress that magnetic island. In other words, if once the magnetic island can be suppressed by reduction of $\Delta\Phi_{\mathrm{RMP}}$, there is latitude to maintain that situation.

4. Discussion

Before entering the discussion, summarised below are behaviours of the magnetic island during the transition observed in the experiment to revisit roles of the RMP and the poloidal flow. First, the island transition from healing to growth is considered. Before the transition, the amplitude of RMP is relatively small and/or significant poloidal flow exists. Consequently, the magnetic island disappears and the phase difference indicates $\Delta\theta_{m=1} = \pi$ (rad), in which the RMP is shielded in order to prevent penetration into the plasma. When the RMP increases over the threshold and/or the poloidal flow decreases, the RMP starts to penetrate leading to the

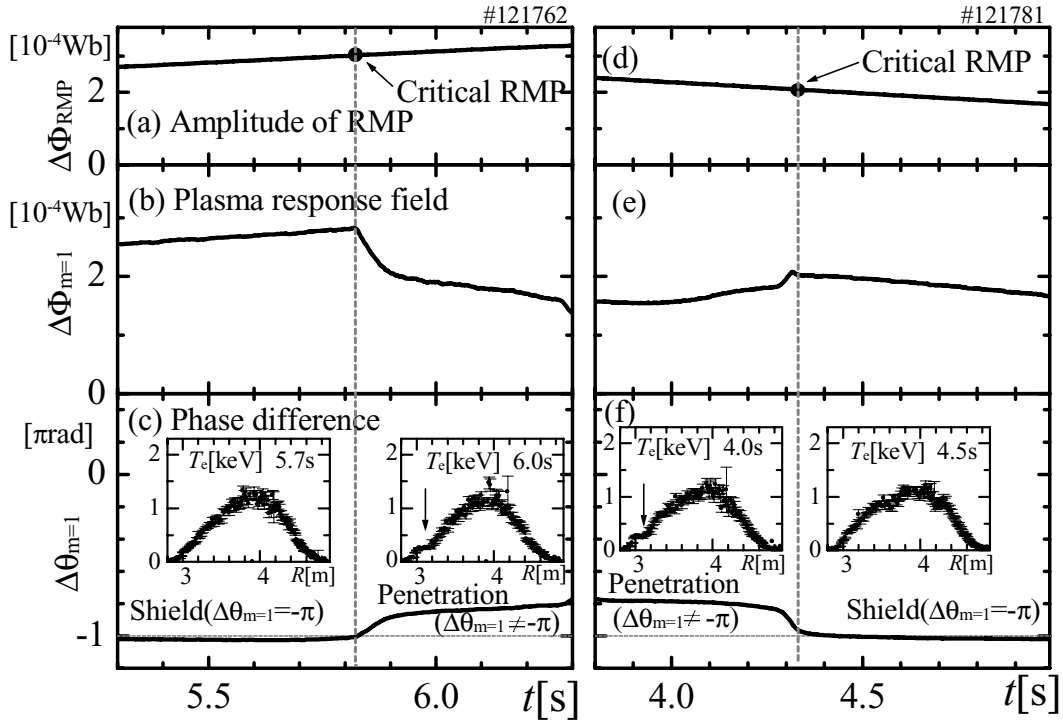

Figure 6. Time evolution of amplitude of RMP $\Delta\Phi_{\mathrm{RMP}}$ (a, d), amplitude of plasma response field $\Delta\Phi_{m=1}$ (b, e) and phase difference $\Delta\theta_{m=1}$ (c, f). (Left) RMP ramp-up case. (Right) Ramp-down case. Electron temperature profiles are shown in (c, f). When RMP is shielded, $\Delta\theta_{m=1}$ indicates out-of phase ($\Delta\theta_{m=1} = -\pi$) and local flattening region does not appear in T_{e} profile whereas local flattening region can be seen in T_{e} profile (indicated arrows) when RMP is penetrated. Threshold of $\Delta\Phi_{\mathrm{RMP}}$ in the ramp-up case is larger than that for the ramp-down case. The vertical dashed lines indicate the time when the RMP reaches the critical value for the transitions.

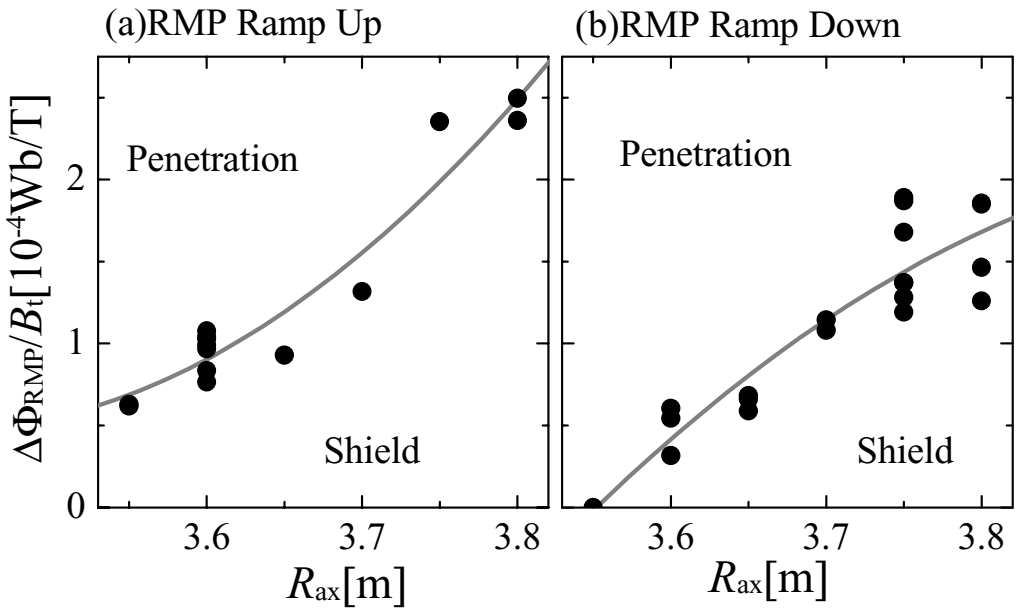

Figure 7. Magnetic axis R_{ax} dependence of critical $\Delta\Phi_{\mathrm{RMP}}$ for ramp-up case (a) and ramp-down case (b), respectively. The region above (below) the gray fitted line corresponds to penetration (shield). In both cases of RMP ramp-up and down, critical $\Delta\Phi_{\mathrm{RMP}}$ increases with R_{ax}.

phase difference moving away from $\Delta\theta_{m=1} = \pi$ (rad). As a result, the magnetic island appears. Second, the behaviour of the opposite transition (island growth to island healing) is as follows. In the case in which the amplitude of the RMP is sufficiently large and/or slow poloidal flow exists, the RMP penetrates into the plasma resulting in the appearance of the magnetic island. When the RMP decreases under the threshold and/or the poloidal flow increases, the RMP is shielded, which leads to the simultaneous disappearance of the island and the phase difference being set to $\Delta\theta_{m=1} = \pi$ (rad).

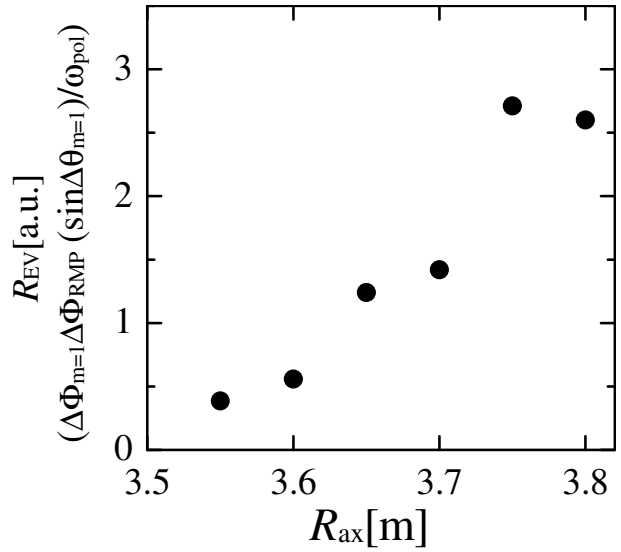

Figure 8. Dependence of the ratio of $\Delta\Phi_{m=1}\Delta\Phi_{RMP}(\sin\Delta\theta_{m=1})$ to $|\omega_{pol}|$ on the magnetic configuration R_{ax}.

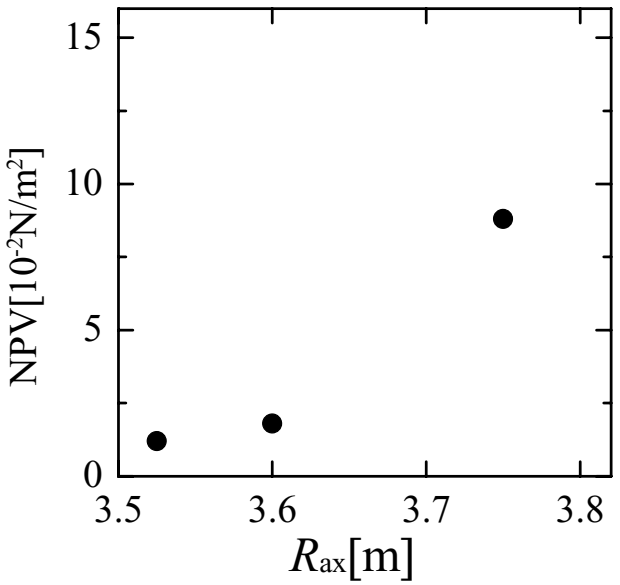

Figure 9. NPV calculated by FORTEC-3D. NPV increases with R_{ax}.

In the theoretical study of the magnetic island [8], the ion-polarisation current leads to the island bifurcation (hysteresis) when that current effect has a stabilising effect. Even though the ion-polarisation current and the motion of the ion (ion-mass flow) cannot be exactly measured experimentally, we use the ω_{pol} measured by CXS presuming the behaviour of the ion flow. These two parameters (RMP and the poloidal flow) are thought to affect the magnetic island as the electromagnetic force and the drag force, respectively. The interaction of these two parameters may be a key mechanism to understand the physics of the island dynamics.

Here, we suppose the interaction between a driving force (for island rotation) and a resisting force (for island locking). The driving force can be considered as a *drag force* on the magnetic island from the poloidal rotation. Here, it should be noted that the terminology of the 'drag' means that the rotating plasma drags the magnetic island to make its velocity increase. The other force is thought to be an electromagnetic force produced by the cross product between the RMP and the modified plasma current making the plasma response field. Using the experimental data, the electromagnetic force F_{EM} and the drag force F_V can be written as $F_{EM} = A_{EM}\Delta\Phi_{m=1}\Delta\Phi_{RMP}(\sin\Delta\theta_{m=1})$ and as $F_V = A_V|\omega_{pol}|$, respectively. Here, A_{EM} and A_V are coefficients or operators which have not been determined yet. The poloidal flow ω_{pol} used here is the extremal value outside the rational surface of $\iota/2\pi = 1$ (see figure 4. The extremal value of ω_{pol} is at $r_{eff} \sim 0.6$). These experimental data are extracted from a condition when the RMP is penetrated because the drag force cannot be defined in which the RMP is shielded. Hereafter, the ratio of the $\Delta\Phi_{m=1}\Delta\Phi_{RMP}(\sin\Delta\theta_{m=1})$ to $|\omega_{pol}|$ is defined as R_{EV}. To clarify the effect of the magnetic configuration (R_{ax}), the relationship between the R_{EV} and R_{ax} is shown in figure 8. The R_{EV} linearly increases with R_{ax}. Apparently, figure 8 does not seem to show that the electromagnetic force F_{EM} and the drag force F_V are balanced. Here, a question arises: what depends on the R_{ax}? The R_{EV} can be supposed to be constant even in the different R_{ax} if these forces are balanced. These experimental observations imply the existence of a hidden parameter.

To find the hidden parameter for the island behaviour, the following are assumed. First, the electromagnetic torque T_{EM} and the drag torque T_V can be written using coefficients of C_{EM} and C_V as $T_{EM} = C_{EM}\Delta\Phi_{m=1}\Delta\Phi_{RMP}(\sin\Delta\theta_{m=1})$ and $T_V = C_V\omega_{pol}$, respectively. Second, these torques are balanced regardless of the R_{ax}, so that $T_{EM}/T_V =$ constant is satisfied. Third, the coefficient of C_{EM} relevant to the magnetic configuration is constant. The electromagnetic torque depends on magnetic shear. This is not greatly different (within 10%) in the range of configuration (R_{ax}) used in this experiment. Furthermore, the effect of the magnetic curvature can be ignored, as mentioned in [10]. Therefore, we assume the C_{EM} is constant in the range of R_{ax} studied here. As a result, the experimentally obtained value of R_{EV} can be written as $R_{EV} = (C_V/C_{EM})\,(T_{EM}/T_V)$.

Revisiting figure 8 with the above assumptions, it can be seen that the change of the R_{EV} originated from the C_V depending on the R_{ax}. The poloidal flow affects the magnetic island as the drag force via the plasma viscosity which would be included in the C_V. Here, the poloidal viscosity is considered as a candidate to explain the R_{EV} depending on the R_{ax}.

The neoclassical poloidal viscosity (NPV) calculated by FORTEC3-D [9] is plotted in figure 9. The NPV increases with R_{ax} similarly to the experimentally obtained R_{EV} which also increases with R_{ax} (figure 8). The behaviour of NPV increasing with R_{ax} implies that the drag force increases at larger R_{ax} via the increase in NPV under the condition of the constant poloidal flow. This picture corresponds to the experimental fact that magnetic islands are likely to be healed at larger R_{ax}. Some theoretical studies [10–13] based on the balance between the electromagnetic torque and the viscous torque have reported that the magnetic island dynamics in the LHD can be explained by the theoretical model of the balance between the electromagnetic torque and the viscous torque. The poloidal viscosity would be a key role to explain the dynamics of the magnetic island in the LHD experiment.

This paper has shown the clear experimental observation of the hysteresis. The phenomena of hysteresis are predicted in some theoretical models based on the balance between the viscous torque and the electromagnetic torque. However, in experiment, the mechanism of hysteresis could not be directly explained by the viscosity because the viscosity cannot be measured in experiment. When we consider the effect of the viscous torque, the behaviour of the viscosity should be estimated experimentally. As the result, the dependence of the viscosity of the R_{ax} can be found as one of the candidates for explaining the dependence of the threshold of RMP to transition on the R_{ax}. From the viewpoint of the experiment, understanding of the mechanism of the hysteresis is thought to be a future subject.

5. Summary

The magnetic island in the LHD has shown the dynamical behaviour. Transition is triggered by the change of RMP and/or poloidal flow. It is observed that thresholds of the amplitude of RMP for the healing/growth transition of the magnetic island depend on magnetic axis position R_{ax}. The RMP threshold increases as the magnetic axis position R_{ax} increases. Furthermore, it was found that the threshold of RMP for healing is smaller than that for growth, which means hysteresis in the critical RMP at a healing/growth transition. The magnetic island response to RMP and its hysteresis have been identified in the LHD. The balance between electromagnetic force and drag force is thought to explain the dynamics of the magnetic island. The poloidal viscosity may be a candidate for the island behaviour in the LHD.

Acknowledgments

The authors thank the LHD operation group for their excellent technical support. One of the authors (Y.N.) wishes to thank Professor K. Ichiguchi who provided fruitful discussion. This study was supported by the budget (ULPP014 and IIDI001) of the NIFS. This work was supported by JSPS KAKENHI Grant Number 15K06649.

References

[1] Waelbroeck F.L. 2009 Theory and observations of magnetic islands *Nucl. Fusion* **49** 104025
[2] Narushima Y. *et al* 2007 Magnetic diagnostics of magnetic island in LHD *Plasma Fusion Res.* **2** S1094
[3] Narushima Y. *et al* 2008 Dependence of spontaneous growth and suppression of magnetic island on beta and collisionality in LHD *Nucl. Fusion* **48** 075010
[4] Sakakibara S. *et al* 2013 Response of MHD stability to resonant magnetic perturbation in the large helical device *Nucl. Fusion* **53** 043010
[5] Narushima Y., Kobayashi M., Akiyama T., Sakakibara S., Masuzaki S., Ashikawa N. and Ohno N. 2013 Behavior of plasma response field in detached plasma *Plasma Fusion Res.* **8** 1402058
[6] Narushima Y. *et al* 2011 Experimental study of poloidal flow effect on magnetic island dynamics in LHD and TJ-II *Nucl. Fusion* **51** 083030
[7] Sakakibara S. and Yamada H. 2010 Magnetic measurements in LHD *Fusion Sci. Technol.* **58** 471
[8] Itoh K., Itoh S.-I. and Yagi M. 2005 Self-sustained annihilation of magnetic islands in helical plasmas *Phys. Plasmas* **12** 072512
[9] Satake S., Sugama H., Kanno R. and Park J.K. 2011 Calculation of neoclassical toroidal viscosity in tokamaks with broken toroidal symmetry *Plasma Phys. Control. Fusion* **53** 054018
[10] Nishimura S., Toda S., Yagi M. and Narushima Y. 2012 Nonlinear stability of magnetic islands in a rotating helical plasma *Phys. Plasmas* **19** 122510
[11] Nishimura S., Toda S., Narushima Y. and Yagi M. 2013 Influence of resonant magnetic perturbation on a rotating helical plasma *Plasma Phys. Control. Fusion* **55** 014013
[12] Hegna C.C. 2011 Healing of magnetic islands in stellarators by plasma flow *Nucl. Fusion* **51** 113017
[13] Hegna C.C. 2012 Plasma flow healing of magnetic islands in stellarators *Phys. Plasmas* **19** 056101